Original Article

Efficacy of shear wave dispersion imaging for viscoelastic assessment of the liver in acute graft-versus-host disease rats

Yu Xiong[1#]^, Yuwei Xin[1#], Feifei Liu[1,2], Wenxue Li[1], Yiqun Liu[1], Jia'an Zhu[1]

[1]Department of Ultrasound, Peking University People's Hospital, Beijing, China; [2]Department of Ultrasound, Binzhou Medical University Hospital, Binzhou, China

Contributions: (I) Conception and design: Y Xiong, Y Xin, Y Liu; (II) Administrative support: J Zhu; (III) Provision of study materials or patients: Y Xiong, Y Xin, Y Liu; (IV) Collection and assembly of data: Y Xiong, Y Xin; (V) Data analysis and interpretation: Y Xiong, Y Xin; (VI) Manuscript writing: All authors; (VII) Final approval of manuscript: All authors.

[#]These authors contributed equally to this work.

Correspondence to: Jia'an Zhu; Yiqun Liu. Department of Ultrasound, Peking University People's Hospital, 11 Xizhimen South Street, Beijing 100044, China. Email: zhujiaan@pkuph.edu.cn; liuyiqunqun1990@163.com.

Background: To investigate the feasibility of using shear wave dispersion (SWD) imaging to evaluate hepatic acute graft-versus-host disease (aGVHD) in a rat model.

Methods: To establish an aGVHD model, 30 Wistar rats were subjected to bone marrow transplantation, 10 Fischer 344 rats were used as donors, and 6 Wistar rats were used as the control group. Each week, 6 rats were randomly chosen and divided into groups of 1 week (1 w) to 5 weeks (5 w). For each subgroup, the rats received a clinical index assessment and shear wave dispersion (SWD) examination with 2 quantitative values, shear wave (SW) speed and SWD slope. The histological characteristics were then used as the reference standard to divide the rats into the aGVHD group and the no aGVHD (nGVHD) group.

Results: In the 2 weeks (2 w) group, only SWD slope [median: 7.26, interquartile range (IQR): 7.04 to 7.31] showed a significant increase in the measured value ($P<0.05$). The value of the 3 weeks (3 w) group (median: 7.88, IQR: 7.84 to 8.49) significantly increased compared with the 2 w value ($P<0.05$). Although the value increased gradually from week 3 to week 5, it had no statistical significance ($P>0.05$). The SW speed [mean ± standard deviation (SD): 1.54±0.11, 95% confidence interval (CI): 1.48 to 1.59] and SWD slope (mean ± SD: 8.29±0.56, 95% CI: 7.99 to 8.59) of the aGVHD group were higher than those of the control group and the nGVHD group ($P<0.001$). The correlation of SWD slope with pathological grade was the highest ($r=0.798$, $P<0.01$), followed by SW speed ($r=0.785$, $P<0.01$), and the correlation of clinical index with pathological grade was the lowest ($r=0.751$, $P<0.01$). In addition, the area under the receiver operating characteristic (ROC) curve (AUC) value of aGVHD using the SWD slope was 0.844 (95% CI: 0.67 to 0.95, sensitivity: 93.75%, specificity: 78.57%), which was higher than the AUC of both SW speed and clinical index, and the difference was statistically significant compared to the AUC of the clinical index.

Conclusions: The SWD slope could show significant abnormalities earlier than SW speed and clinical index and is also more consistent with the change in aGVHD severity level. The SWD slope may help in detecting hepatic aGVHD during ultrasound SWD examination.

Keywords: Acute graft-versus-host disease (aGVHD); liver; shear wave elastography; shear wave dispersion slope

Submitted Apr 14, 2022. Accepted for publication Aug 14, 2022.
doi: 10.21037/qims-22-374
View this article at: https://dx.doi.org/10.21037/qims-22-374

^ ORCID: 0000-0002-7499-7785.

Introduction

Acute and chronic graft-versus-host disease (GVHD) are serious complications after allogeneic hematopoietic stem cell transplantation (allo-HSCT) (1-3). Acute graft-versus-host disease (aGVHD) usually occurs 10–100 days after allo-HSCT and has a prevalence of 30–50% (4,5). As one of the leading causes of early nonrecurrent death after allo-HSCT surgery, aGVHD seriously affects patients' prognosis and survival rate (3,6). The liver is one of the primary organs targeted by aGVHD (3). Early diagnosis and symptomatic treatment are crucial to the clinical outcome of patients with hepatic aGVHD. Delaying the use of immunosuppressive agents, particularly corticosteroids, may reduce postoperative survival (1,3,6). However, hepatic aGVHD is primarily diagnosed based on clinical manifestations and a nonspecific laboratory examination (7). Although a liver biopsy can help with diagnosis, it is an invasive procedure and difficult to apply to patients with severe disease and those with severe thrombocytopenia (8).

Shear wave elastography (SWE) is a noninvasive technique that assesses tissue elasticity through the propagation of shear waves. The velocity of shear waves (SW) in tissue increases with increasing tissue stiffness (9). Previous studies have reported wide use of SWE to assess liver stiffness (10,11). After allo-HSCT, elastography has been demonstrated to improve the accuracy of early diagnosis of hepatobiliary complications (12). The SWE method may serve as a promising and viable risk prediction tool for predicting liver events and overall mortality in the first year following allogeneic stem cell transplantation (13,14).

In clinical applications, most SWE models use linear elastic models to describe the mechanical properties of tissue through quantification of the elasticity of tissues, ignoring the viscosity of tissues (15-17). When a shear wave propagates in viscoelastic tissue, its speed depends on frequency, which is the frequency dispersion of the shear wave (15,17,18). The resulting dispersion phenomenon is related to the viscosity of tissue. Liver tissue is viscoelastic tissue with dispersion properties, and the speed of shear waves increases with frequency (16,19). As a result, SWE dispersion analysis can be used as an indirect method to measure the viscosity of the liver. Recently, a new ultrasound (US) elastography method based on the analysis of the shear wave dispersion (SWD) slope has been able to quantitatively measure SW speed related to viscoelasticity and SWD slope related to viscosity (17). Previous studies have applied this method to assess nonalcoholic fatty liver disease (20,21). Furthermore, studies suggest that SWD slope, as a new noninvasive method, has potential value in evaluating liver disease activity in primary biliary cholangitis (22). However, to date, no study has been conducted to apply SWD imaging to hepatic aGVHD.

The pathological mechanism of aGVHD is an inflammatory reaction, mainly involving lymphocyte infiltration and damage to bile ducts as well as portal inflammation (23). Previous research has suggested that SWD slope is a better predictor of necrotic inflammation than SW speed (17,18). In this study, it was assumed that changes in the pathophysiological characteristics of hepatic aGVHD would mainly lead to an increase in the SWD slope, potentially enabling SWD imaging to provide noninvasive quantitative diagnosis of hepatic aGVHD. Therefore, the purpose of this study was to prospectively evaluate the role of SWD imaging in the assessment of live aGVHD. We present the following article in accordance with the Animal Research: Reporting of In Vivo Experiments (ARRIVE) reporting checklist (available at https://qims.amegroups.com/article/view/10.21037/qims-22-374/rc).

Methods

Model establishment of aGVHD

In this study, 45 female Wistar rats (Beijing Vital River Laboratory Animal Technology, Beijing, China), aged 6–8 weeks and weighing 180–200 g, and 10 male Fischer 344 rats (n=10) were selected. All Wistar rats were numbered by another researcher, and the standard =RAND () function in Microsoft Excel (Microsoft Corp., Redmond, WA, USA) was used to generate random numbers. Six normal Wistar rats were randomly selected as the control group (n=6); the remaining Wistar rats served as bone marrow transplantation recipients to establish an aGVHD model (24), and the 10 Fischer 344 rats were used as the donors. Rats were housed in sterile isolation cages with constant temperature and humidity and a 12-h light/dark cycle. The rats had unlimited access to water and food. All experimental procedures involving animals were approved by the Institutional Animal Care and Use Committee of Peking University People' s Hospital (License number: 2020PHE088). All experiments were performed according to the Guide for the Care and Use of Laboratory Animals.

Fischer 344 rats were euthanized with 5% isoflurane, and bone marrow (BM) was removed from the femurs and

tibias with a 26-gauge needle and flushed with cold Roswell Park Memorial Institute (RPMI) 1640. The BM cells were then centrifuged for 5 minutes at 1,000 rpm to pellet them. A 3 mL Pasteur pipette was used to resuspend BM cells gently, followed by filtration through a nylon filter with a mesh size of 200. Trypan blue exclusion test of cell viability determined that the viability was >95% consistent.

Splenectomy was performed under sterile conditions. The spleens of Fischer 344 rats were cut into small pieces, and fragments were crushed between 2 glass slides in medium and then collected and suspended in cold RPMI 1640. Filtered spleen cell suspensions were washed 3 times with cold RPMI 1640 and filtered through a 200-mesh nylon filter. Trypan blue exclusion test of cell viability revealed that splenocyte viability was >95% consistent. With an injection of 4×10^7 donor splenocytes, we created an aGVHD rat model in the context of allo-HSCT. The 4×10^7 donor splenocytes were mixed with 4×10^7 BM cells, then diluted in 0.5 mL phosphate-buffered saline (PBS), and subsequently administered through tail veins to female Wistar rats. Before allo-HSCT, the recipient rats received a myeloablative treatment that included 8 Gy of total body irradiation. The same individual performed all experiments to avoid operator-to-operator interaction. In addition, all experimental procedures were conducted in accordance with the principles of sterility.

After allo-HSCT, 6 rats were randomly selected from the model rats each week until the fifth week (5 w) for *in vivo* SWD examination. The rats were euthanized at the end of the examination and then underwent histopathological examination *in vitro* (17,25). Rats that died following transplantation immunosuppression or whose pathological manifestations were primarily hepatic sinus injury supporting the diagnosis of sinusoidal obstruction syndrome (SOS) were excluded from the experiment (26).

Clinical observation

A standard scoring method was used to determine the severity of systemic aGVHD (27), which included 5 clinical parameters: weight loss, posture (hunching), activity, fur texture, and skin integrity. Each parameter was assessed and classified on a scale of 0 to 2: weight loss (0: <10%; 1: 10–25%; 2: >25%), posture (0: normal; 1: hunchback is only observed at rest; 2: movement for severe hunchback impairment), activity (0: normal; 1: mild to moderate decline; 2: only active when stimulated), fur texture (0: normal; 1: mild to moderate wrinkles; 2: severe wrinkles), and skin integrity (0: normal; 1: paw/tail scaling; 2: obvious exposed skin area). The sum of the 5 standard scores produced a clinical index (maximum index =10).

SWD examination

An experienced US abdominal sonographer examined each rat at specified times. The machine used for the experiment was an ultrasound scanner (Aplio i800; Canon Medical Systems Corporation, Otawara, Tochigi, Japan) equipped with a linear array transducer (18 MHz) and in accordance with guidelines proposed by the World Federation of Societies for Ultrasound in Medicine and Biology and the European Federation of Societies for Ultrasound in Medicine and Biology (28,29).

Before US exams, rats were anesthetized by intraperitoneal injection with a ketamine/xylazine mix (60 mg/kg ketamine, 7.5 mg/kg xylazine). During anesthesia, the needle was inserted into the lower abdomen far from the liver, and back extraction was performed before each injection to ensure that no abdominal organs or blood vessels were injured. The rats were placed on a heating pad in the supine position, and the abdomen was shaved to fully expose the abdominal skin and then coated with an adequate amount of ultrasonic couplants. The operator selected the ideal acoustic window in the abdominal region as much as possible without artifacts caused by ribs and gas. An approximately 1×1 cm sample box was placed roughly 1.0–1.3 cm beneath the capsule on a grayscale picture. The SWD ultrasound image was then activated, and the machine automatically displayed a twin view of the grayscale map and shear wave propagation map, after which it switched into quad-view mode, comprising 4 maps (SW speed map, propagation map, grayscale map, and SWD slope map). After cooling for 5 s to stabilize the SWD image, the image was captured and saved. Since each pair of photographs was interlocked, the SW speed and SWD slope values were obtained simultaneously by placing the region of interest (ROI) on the map. A 2 mm circular ROI was inserted in the liver parenchyma using the propagation map as a guide, avoiding major arteries and the transducer's compression impact (*Figure 1*). A total of 15 measurements were obtained by measuring SW speed and SWD slope 3 times from 5 separate images to increase repeatability, and the mean value was selected for subsequent analysis. Two operators with more than 10 years of experience in abdominal US and more than 5 years of experience in elastography performed all SWD measurements independently. In addition,

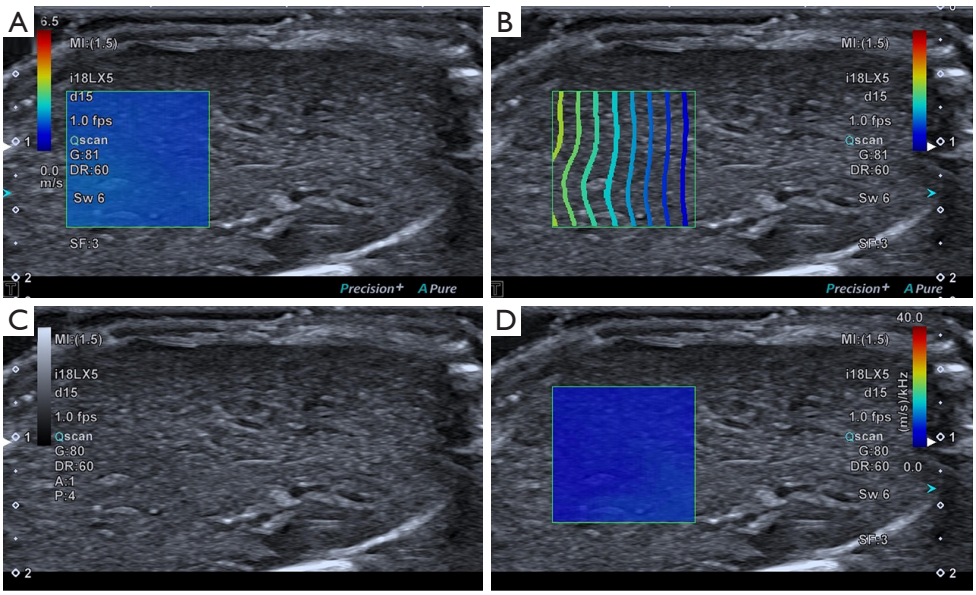

Figure 1 Quad-view of SWD imaging of the liver. (A) SW speed map. (B) Propagation map. (C) Grayscale map. (D) SWD slope map. SWD, shear wave dispersion; SW, shear wave.

operator 1 performed a second measurement 30 minutes after the initial examination, and operator 2 performed the measurement in the same manner, with no regard to the measurement results of the first operator. The measurement results of operator 1 were used in subsequent statistical analyses.

Histopathological analysis

After completing the sonography, rats were sacrificed with an overdose of pentobarbital (75 mg/kg) via intraperitoneal injection. The liver was then dissected, sectioned as accurately as possible on the same plane as SWD images, fixed in 20% neutral-buffered formalin for 24–72 h, and encased in paraffin. A formalin-fixed paraffin-embedded tissue sample was then used to generate 3 μm-thick tissue sections, which were placed on glass slides and stained with hematoxylin and eosin (H&E). All histopathological examinations were performed by pathologists with 10 years of experience in liver pathological analysis. A 5-point scale was used for semiquantitative grading of aGVHD in H&E-stained slides: grade 0 (none); grade 1 (slight: slight inflammation of the portal triads or lobule); grade 2 (mild: mild inflammation of the portal triads or lobule); grade 3 (moderate: bile duct lymphocytic infiltration and bile duct damage with portal inflammation; and grade 4 (severe: lymphocytic infiltration of bile duct, damage or loss of bile duct, and cholestasis with portal inflammation), as shown in *Figure 2*. When the pathogenic index of the grading method was above 2 (moderate and severe), aGVHD was identified (30-32). These rats comprised the aGVHD group, and the rats with pathological grades not meeting the diagnostic criteria were grouped as the no aGVHD (nGVHD) after transplantation group.

Statistical analysis

The software MedCalc (version 20-64 bit; MedCalc, Ostend, Belgium) and SPSS 23.0 (IBM Corp., Armonk, NY, USA) were used for statistical analysis. Normal distribution of data was checked using the Shapiro-Wilk test. Data conforming to normal distribution were compared among groups using one-way analysis of variance (ANOVA). The least significant difference (LSD) test was used for post-hoc analysis. Results are expressed as mean and standard deviation (SD). The Jonckheere–Terpstra test was used for data that did not conform to normal distribution. Results were expressed as median, first quartile, and third quartile. The association between histological grades and SW speed, SWD slope, and the clinical index was investigated using Spearman's correlation analysis. The intraclass correlation coefficient (ICC) calculated by the two-way random-effects

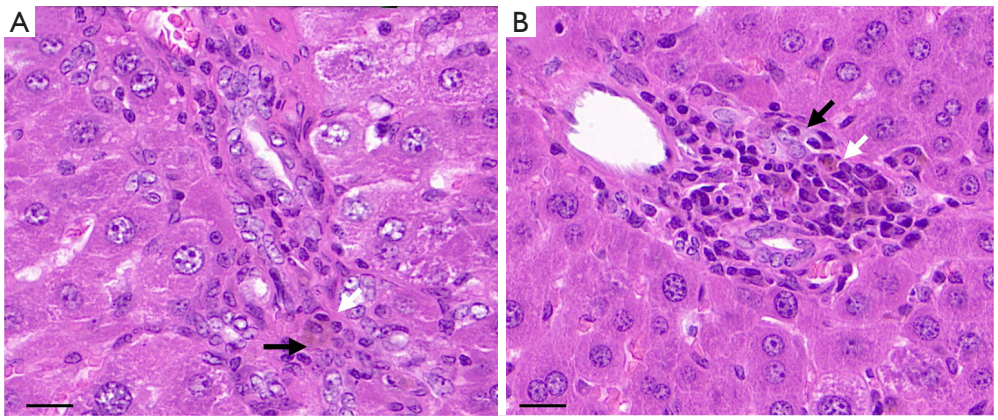

Figure 2 Histopathologic evaluation of rat livers. (A) The bile duct cells are disorderly arranged (black arrow) and infiltrated with inflammatory cells (white arrow). The pathological grade was 3. (B) The bile duct cells are damaged (black arrow), with cholestasis and a large number of infiltrated inflammatory cells in the periphery (white arrow). The pathological grade was 4. H&E staining magnification: ×400, scale bar 20 μm. H&E, hematoxylin and eosin.

model was used to evaluate the consistency of SW speed and SWD slope values between and within observers. The performance of SW speed, SWD slope, and the clinical index in identifying aGVHD was determined using receiver operating characteristic (ROC) curve analysis. The DeLong *et al.* test was used to calculate the area under the ROC curve (AUC), and these methods were then compared (33).

Results

Model establishment results

A total of 9 rats were excluded from this study, including 1 with a pathological manifestation of SOS, 4 that died from immunosuppressive infection after allo-HSCT, and 4 that died from anesthetic overdose. Finally, 30 Wistar rats were included in the experiment, including 16 with a pathological diagnosis of aGVHD in the aGVHD group and 14 with a pathological score of 2 or less in the nGVHD group.

After allo-HSCT, only weight loss occurred in the 1 w [median: 3.50, interquartile range (IQR): 3.00 to 4.00] and 2 w groups (median: 3.50, IQR: 3.00 to 4.00), significantly increasing the clinical index from that of the control group (P<0.05). In the 3 w group, clinical manifestations such as an arched back, decreased mobility, and alopecia began to appear, and the clinical index (median: 6.00, IQR: 4.78 to 8.00) increased significantly compared with that of the 2 w group, as shown in *Figure 3* and *Table 1* (P<0.05). The clinical indices of the 4 w and 5 w groups continued to increase, but there was no significant difference between them and the 3 w group (P>0.05).

Histopathological analysis

The distribution of pathological grades in each group are demonstrated in *Figure 4*. After allo-HSCT, the pathological grade gradually increased, no significant changes were observed in the liver of the 1 w group (P>0.05), portal vein infiltration and hepatocyte deformation occurred in the 2 w group, and pathological grades (median: 2.00, IQR: 1.75 to 2.25) were significantly higher than the control group and 1 w group (median: 0, IQR: 0 to 1.00) (P<0.05). In the 3–5 w groups, the pathological changes were worse, except for portal vein inflammation and damage to the bile duct cells. There was no significant difference in pathological grades between the 3 groups (P>0.05), and the scores were significantly higher than those in the 2-w group (P<0.05).

SWD examination

The US values of each group are shown in *Figure 5* and *Table 1*. The SW speed and SWD slope values rose over time compared to the control group, as shown in *Figure 6*. The 1 w group did not significantly differ in SW speed or SWD slope (P>0.05). There was no significant increase in SW speed in the 2 w group (median: 1.38, IQR: 1.29 to 1.39) (P>0.05), but SWD slope values were significantly higher (median: 7.26, IQR: 7.04 to 7.31) (P<0.05). The SW speed and SWD slope values of the 3–5 w groups

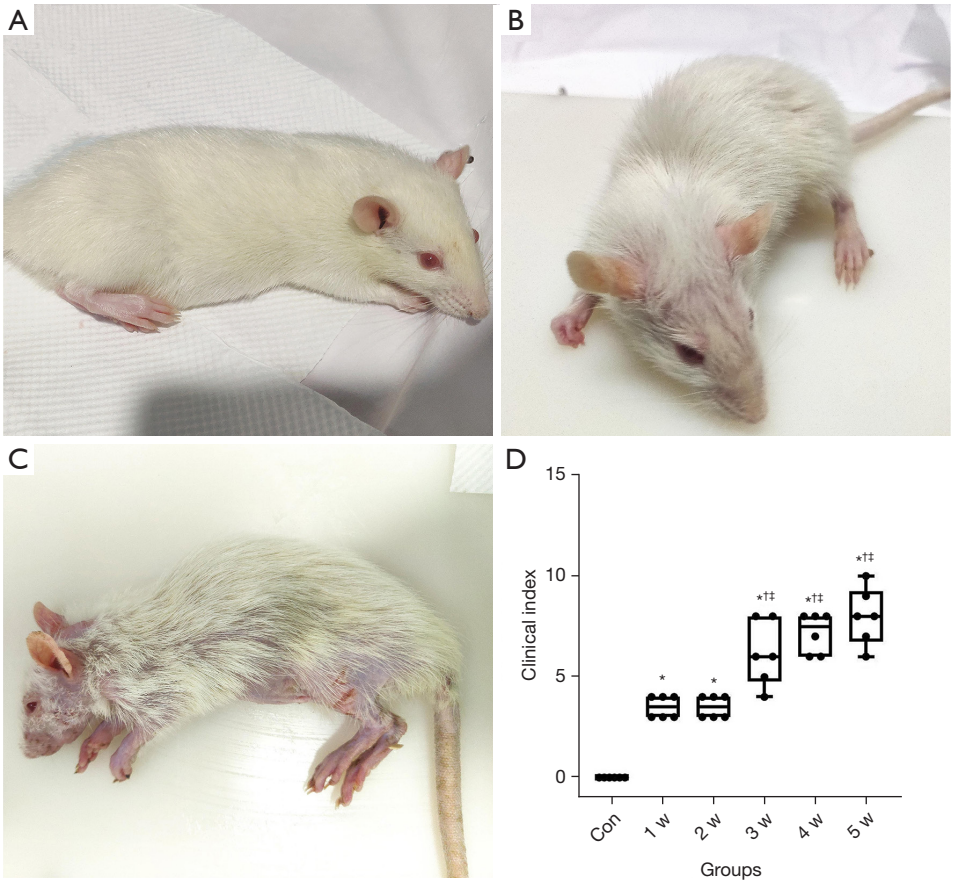

Figure 3 Clinical manifestations and clinical index of rats. (A) The rats in the 1 w group only lost weight and did not show other clinical symptoms. (B) In the 2 w group, the rats showed slight hunchback and local alopecia. (C) The rats in the 5 w group had severe hunched back, decreased activity, obvious systemic alopecia, and multiple scabs on the skin. (D) Boxplots showing the distribution of clinical indices for each group. *P<0.05 versus the control group; †P<0.05 versus the 1 w group; ‡P<0.05 versus the 2 w group. Con, control group; w, week.

Table 1 Pathological, ultrasonic, and clinical index of livers from the 6 groups (median and interquartile range)

Groups	Pathological grade	Clinical index	SW speed (m/s)	SWD slope, (m/s)/kHz
Con	0 (0)	0 (0)	1.29 (1.20–1.34)	5.95 (5.50–6.32)
1 w	0 (0–1.00)	3.50 (3.00–4.00)*	1.28 (1.23–1.31)	6.06 (5.86–6.13)
2 w	2.00 (1.75–2.25)*†	3.50 (3.00–4.00)*	1.38 (1.29–1.39)	7.26 (7.04–7.31)*†
3 w	3.50 (3.00–4.00)*†‡	6.00 (4.78–8.00)*†‡	1.57 (1.51–1.64)*†‡	7.88 (7.84–8.49) *†‡
4 w	4.00 (2.75–4.00)*†	7.50 (6.00–8.00)*†‡	1.65 (1.55–1.67)*†‡	8.04 (7.85–8.51) *†‡
5 w	3.50 (2.00–4.00)*†	8.00 (6.75–9.25)*†‡	1.48 (1.44–1.55)*†‡	8.99 (8.67–9.19) *†‡

†P<0.05 versus the 1 w group; ‡P<0.05 versus the 2 w group; *P<0.05 versus the control group. SW, shear wave; SWD, shear wave dispersion; Con, control group; w, week.

increased continuously (P<0.05), but there was no significant difference among the 3 groups (P>0.05). The SWD measurements provided excellent interobserver and intraobserver consistency. For interobserver variability in SW speed and SWD slope values, the ICC was 0.816 (95% CI: 0.64 to 0.91) and 0.838 (95% CI: 0.68–0.92), respectively. For intraobserver variability in SW speed and SWD slope values, the ICC was 0.801 (95% CI: 0.61 to 0.90) and 0.823 (95% CI: 0.65 to 0.91), respectively.

There were significant differences in SW speed and SWD slope among the control group, nGVHD group, and aGVHD group (P<0.001). In the pairwise comparison, SW speed in nGVHD group (mean ± SD: 1.38±0.15, 95% CI: 1.29 to 1.46) was not significantly different from that in the control group (mean ± SD: 1.27±0.08, 95% CI: 1.19 to 1.36), but SWD slope (mean ± SD: 7.00±1.11, 95% CI: 6.36 to 7.64) was significantly higher than that in the control group (mean ± SD: 5.92±0.42, 95% CI: 5.48 to 6.35). The aGVHD group's SW speed (mean ± SD: 1.54±0.11, 95% CI: 1.48 to 1.59) and SWD slope (mean ± SD: 8.29±0.56, 95% CI: 7.99 to 8.59) were significantly higher than those of the nGVHD and control groups.

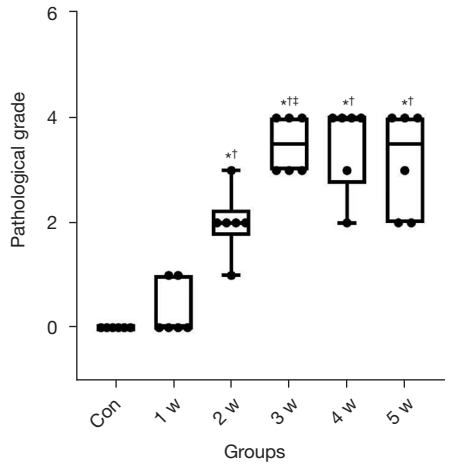

Figure 4 Boxplots showing the distribution of pathological grades (median and quartile range) for each group. *P<0.05 versus the control group; †P<0.05 versus the 1 w group; ‡P<0.05 versus the 2 w group. Con, control group; w, week.

Correlation analysis

The results revealed that histological grades had a significant positive correlation with SW speed, SWD slope, and clinical index (r=0.785, P<0.01; r=0.798, P<0.01; r=0.751, P<0.01).

Diagnostic performance of each variable in detecting aGVHD of the liver

The AUCs for SW speed, SWD slope, and the clinical index to detect aGVHD were 0.810 (95% CI: 0.63 to 0.93), 0.844 (95% CI: 0.67 to 0.95), 0.748 (95% CI: 0.56 to 0.89),

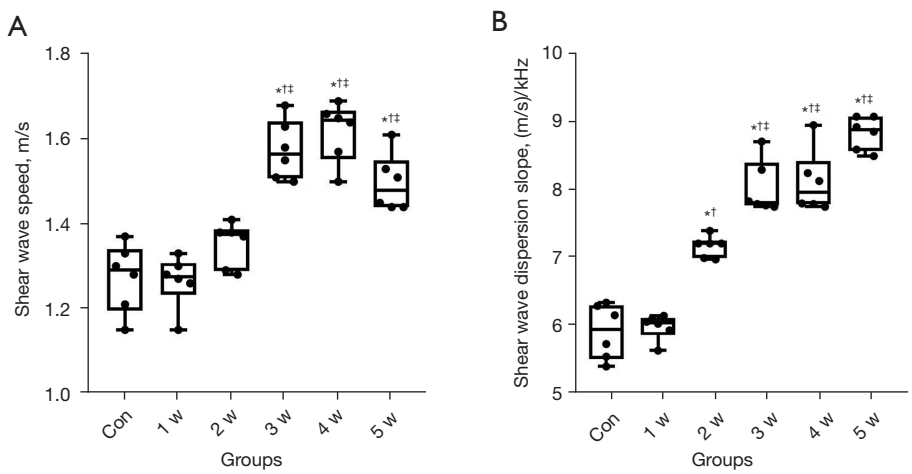

Figure 5 Boxplots showing SWD results (median and interquartile range) for each group. (A) SW speed. (B) SWD slope. *P<0.05 versus the control group; †P<0.05 versus the 1 w group; ‡P<0.05 versus the 2 w group. SWD, shear wave dispersion; SW, shear wave; Con, control group; w, week.

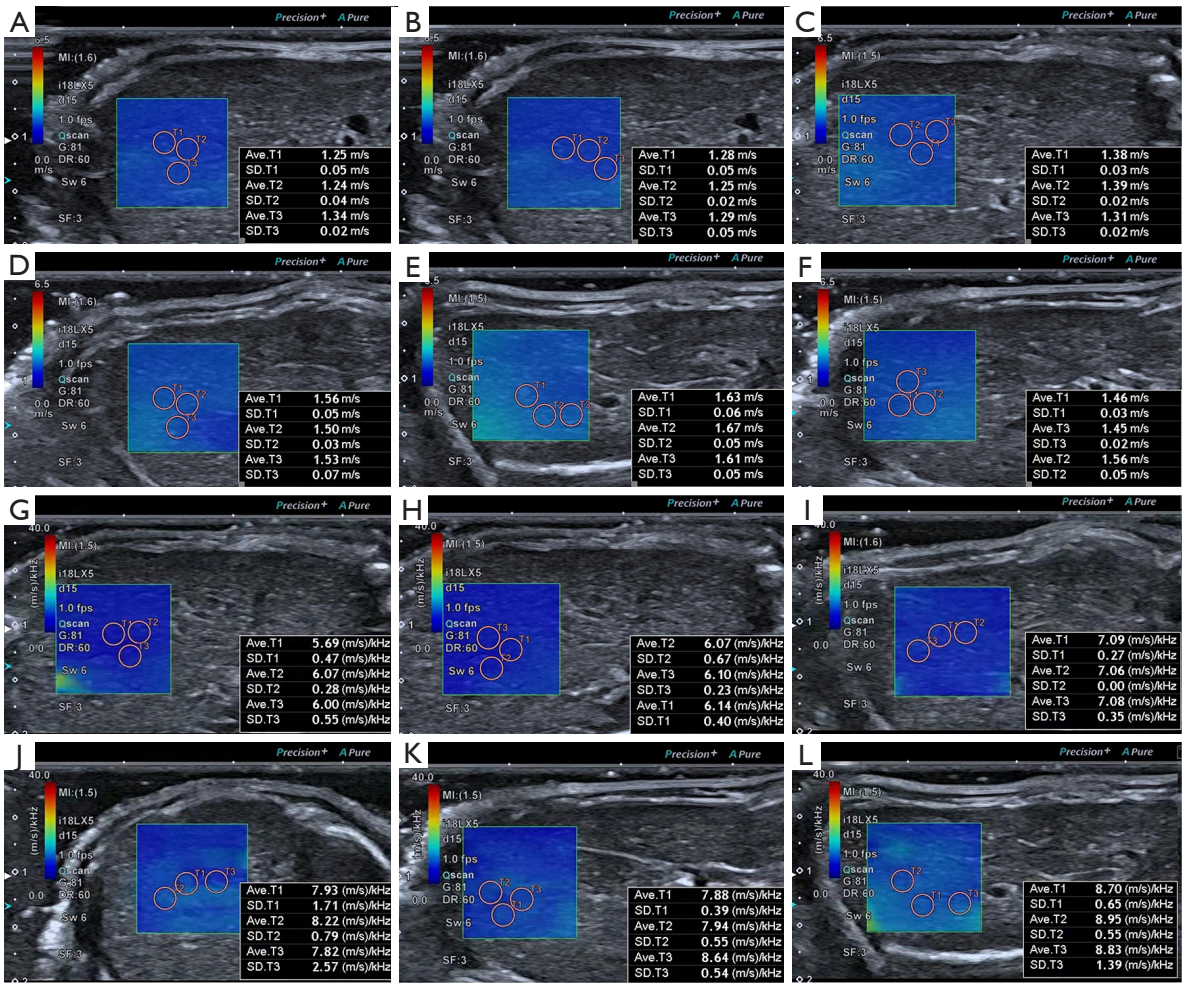

Figure 6 SW speed and SWD slope findings of the liver in normal rats and aGVHD rats. (A,G) The liver of normal rats. (B,H) The liver of the rats after allo-HSCT for 1 week. (C,I) The liver of the rats after allo-HSCT for 2 weeks. (D,J) The liver of the rats after allo-HSCT for 3 weeks. (E,K) The liver of the rats after allo-HSCT for 4 weeks. (F,L) The liver of the rats after allo-HSCT for 5 weeks. SW, shear wave; SWD, shear wave dispersion; aGVHD, acute graft-versus-host disease; allo-HSCT, allogeneic hematopoietic stem cell transplantation.

respectively, as shown in *Figure* 7. The difference in AUC between SWD slope and the clinical index was statistically significant ($P<0.05$). The cut-off value of the SWD slope selected by maximizing the Youden index was 7.45, sensitivity was 93.75%, and specificity was 78.57%.

Discussion

The new ultrasonic technology used in this study could provide SW speed values related to viscoelasticity and SWD slope values related to tissue viscosity (17,18,34). Both elasticity and viscosity can provide biochemical information about tissue quality (18). Liver tissue is viscoelastic, with both viscous and elastic properties. The SWD slope can provide quantitative parameters related to viscosity and indirectly reflect the changing trend of viscosity (15,18). Previous studies have demonstrated that inflammatory response in the liver may be more related to SWD slope, and that fibrosis is more related to SW speed (17,18,25). Given that GVHD is an inflammatory response (30,31,35), SWD slope may be a more valuable diagnostic method in aGVHD than SW speed.

This study found that during the second week, the SWD slope could be abnormal concurrently with a pathological grade and be significantly increased at the time of pathological aggravation in the third week. However,

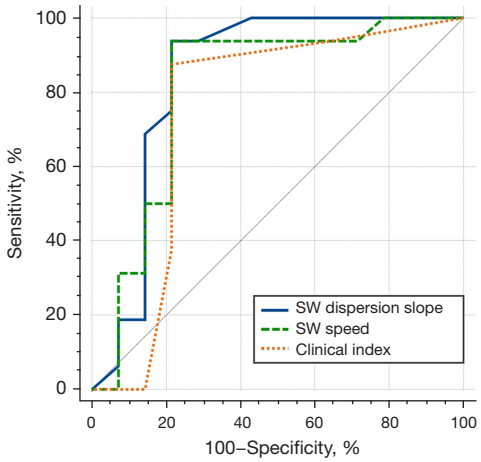

Figure 7 ROC curves for detection of hepatic aGVHD using SW speed, SWD slope, and clinical index. aGVHD, acute graft-versus-host disease; ROC, receiver operating characteristic; SW, shear wave; SWD, shear wave dispersion.

SW speed and the clinical index did not appear abnormal in the second week and increased significantly in the third week. This might be related to the pathological changes in the liver after allo-HSCT. The livers of the rats included in our study were graded pathologically. Although a liver with a score of less than or equal to 2 could not be diagnosed with aGVHD, and there were no lymphocytes infiltrating the bile ducts or bile duct damage, different degrees of the inflammatory reaction occurred in the portal. Therefore, the SWD slope may be a more effective indicator for predicting the degree of inflammation than SW speed, which is consistent with the results of previous studies (15,17,18,34). In addition, the clinical index increased due to bodyweight loss from the first week, without other clinical manifestations such as hunching and alopecia, until the third week. In combination with the results of a previous study, this situation was considered as body weight loss after irradiation (36).

To eliminate the confounding factor caused by operational toxicity in this study, the rats after allo-HSCT were further divided into 2 groups based on pathological score (aGVHD and nGVHD) and compared with the control group. The results showed that both SW speed and SWD slope were significantly higher in the aGVHD group compared to the control group. The pathological mechanism of aGVHD is mainly inflammatory reactions, including lymphocyte infiltration into the bile ducts, damage or even loss of bile duct cells, and cholestasis, possibly accompanied by portal vein inflammation (30,31,35). Intrahepatic inflammatory responses may lead to edema, which increases the internal pressure of the liver and thus hepatic viscoelasticity, indirectly showing the increase of SWD slope. In recent years, SW speed has been widely used for the measurement of liver stiffness (9,12). Studies have shown that SW speed was affected by fibrosis and may also be increased due to inflammation and necrosis (17,20,34). Compared to the control group, only the SWD slope showed a significant increase in nGVHD, but there was no significant difference in SW speed. This further confirmed that the SWD slope could be a more effective indicator for predicting the degree of inflammation than the SW speed (17,18,34).

In the correlation analysis with pathological grades, the SWD slope showed a better correlation than SW speed and clinical index. In addition, SWD slope provided better diagnostic performance in detecting aGVHD than SW speed and clinical index. In particular, the difference in diagnostic performance between SWD slope and the clinical index was statistically significant. Based on the results of our study, we consider the SWD a valuable noninvasive method for evaluating hepatic aGVHD. The SWD slope is superior to SW speed in detecting hepatic aGVHD.

Although this study had some insightful findings, it also had a few limitations. The sample size was relatively small, and despite that we have obtained some preliminary results, more research with a larger sample size is required in the future. The experimental subjects were rats whose posture and breathing coordination could not be controlled to achieve the best acoustic window. When studying the liver *in vivo*, the movement caused by vascular pulsation and breathing affected the measurement results. However, this may be ignored in most cases as researchers manually modified their posture to achieve better exposure. These movements are low frequency under anesthesia, and SW speed and SWD slope can be obtained quickly. Finally, since this was an animal study, the results cannot be directly translated into clinical practice. Further experimental and clinical studies may be necessary to verify our findings in the future.

Conclusions

This study successfully applied SWD imaging technology to simultaneously obtain SW speed and SWD slope measurements in an animal model of aGVHD of the liver. Using SWD imaging technology, SW speed, and SWD

slope could help to detect the aGVHD of the liver. The SWD slope had better performance in detecting aGVHD groups earlier and reflecting the severity of the disease.

Acknowledgments

Funding: This study was funded by the Youth Project of the National Natural Science Foundation of China (No. 82001826).

Footnote

Reporting Checklist: The authors have completed the ARRIVE reporting checklist. Available at https://qims.amegroups.com/article/view/10.21037/qims-22-374/rc

Conflicts of Interest: All authors have completed the ICMJE uniform disclosure form (available at https://qims.amegroups.com/article/view/10.21037/qims-22-374/coif). The authors have no conflicts of interest to declare.

Ethical Statement: The authors are accountable for all aspects of the work in ensuring that questions related to the accuracy or integrity of any part of the work are appropriately investigated and resolved. The study was approved by the Animal Care and Use Committee of Peking University People's Hospital (No. 2020PHE088). All experiments were performed according to the Guide for the Care and Use of Laboratory Animals.

References

1. Jagasia M, Arora M, Flowers ME, Chao NJ, McCarthy PL, Cutler CS, et al. Risk factors for acute GVHD and survival after hematopoietic cell transplantation. Blood 2012;119:296-307.
2. Lee SE, Cho BS, Kim JH, Yoon JH, Shin SH, Yahng SA, Eom KS, Kim YJ, Kim HJ, Lee S, Min CK, Cho SG, Kim DW, Lee JW, Min WS, Park CW. Risk and prognostic factors for acute GVHD based on NIH consensus criteria. Bone Marrow Transplant 2013;48:587-92.
3. Aladağ E, Kelkitli E, Göker H. Acute Graft-Versus-Host Disease: A Brief Review Turk J Haematol 2020;37:1-4.
4. Chao NJ. Graft-versus-host disease: the viewpoint from the donor T cell. Biol Blood Marrow Transplant 1997;3:1-10.
5. Naserian S, Leclerc M, Shamdani S, Uzan G. Current Preventions and Treatments of aGVHD: From Pharmacological Prophylaxis to Innovative Therapies. Front Immunol 2020;11:607030.
6. Goker H, Haznedaroglu IC, Chao NJ. Acute graft-vs-host disease: pathobiology and management. Exp Hematol 2001;29:259-77.
7. Ali AM, DiPersio JF, Schroeder MA. The Role of Biomarkers in the Diagnosis and Risk Stratification of Acute Graft-versus-Host Disease: A Systematic Review. Biol Blood Marrow Transplant 2016;22:1552-64.
8. Ruggiu M, Bedossa P, Rautou PE, Bertheau P, Plessier A, Peffault de Latour R, Robin M, Sicre de Fontbrune F, Pagliuca S, Villate A, Xhaard A, Socié G, Michonneau D. Utility and Safety of Liver Biopsy in Patients with Undetermined Liver Blood Test Anomalies after Allogeneic Hematopoietic Stem Cell Transplantation: A Monocentric Retrospective Cohort Study. Biol Blood Marrow Transplant 2018;24:2523-31.
9. Chen S, Urban MW, Pislaru C, Kinnick R, Zheng Y, Yao A, Greenleaf JF. Shearwave dispersion ultrasound vibrometry (SDUV) for measuring tissue elasticity and viscosity. IEEE Trans Ultrason Ferroelectr Freq Control 2009;56:55-62.
10. Yang L, Ling W, He D, Lu C, Ma L, Tang L, Luo Y, Chen S. Shear wave-based sound touch elastography in liver fibrosis assessment for patients with autoimmune liver diseases. Quant Imaging Med Surg 2021;11:1532-42.
11. Schulz M, Choi M, Bachmann F, Koch N, Holtmann TM, Mohr R, Tacke F, Wree A. Shear wave elastography-based liver fibrosis assessment in patients with chronic hepatitis E displays elevated liver stiffness regardless of previous antiviral therapy. Quant Imaging Med Surg 2022;12:3528-38.
12. Debureaux PE, Bourrier P, Rautou PE, Zagdanski AM, De Boutiny M, Pagliuca S, Sutra Del Galy A, Robin M, Peffault de Latour R, Plessier A, Sicre de Fontbrune F, Xhaard A, de Lima Prata PH, Valla D, Socié G, Michonneau D. Elastography improves accuracy of early hepato-biliary complications diagnosis after allogeneic stem cell transplantation. Haematologica 2021;106:2374-83.
13. Karlas T, Weiße T, Petroff D, Beer S, Döhring C, Gnatzy F, Niederwieser D, Behre G, Mössner J, Fischer J, Tröltzsch

M, Wiegand J, Keim V, Franke GN. Predicting hepatic complications of allogeneic hematopoietic stem cell transplantation using liver stiffness measurement. Bone Marrow Transplant 2019;54:1738-46.
14. Modi D, Ye JC, Surapaneni M, Singh V, Chen W, Jang H, Deol A, Ayash L, Alavi A, Ratanatharathorn V, Uberti JP. Liver Graft-Versus-Host Disease is associated with poor survival among allogeneic hematopoietic stem cell transplant recipients. Am J Hematol 2019;94:1072-80.
15. Rus G, Faris IH, Torres J, Callejas A, Melchor J. Why Are Viscosity and Nonlinearity Bound to Make an Impact in Clinical Elastographic Diagnosis? Sensors (Basel) 2020;20:2379.
16. Chen S, Urban MW, Pislaru C, Kinnick R, Greenleaf JF. Liver elasticity and viscosity quantification using shearwave dispersion ultrasound vibrometry (SDUV). Annu Int Conf IEEE Eng Med Biol Soc 2009;2009:2252-5.
17. Sugimoto K, Moriyasu F, Oshiro H, Takeuchi H, Yoshimasu Y, Kasai Y, Furuichi Y, Itoi T. Viscoelasticity Measurement in Rat Livers Using Shear-Wave US Elastography. Ultrasound Med Biol 2018;44:2018-24.
18. Sugimoto K, Moriyasu F, Oshiro H, Takeuchi H, Yoshimasu Y, Kasai Y, Itoi T. Clinical utilization of shear wave dispersion imaging in diffuse liver disease. Ultrasonography 2020;39:3-10.
19. Barry CT, Hah Z, Partin A, Mooney RA, Chuang KH, Augustine A, Almudevar A, Cao W, Rubens DJ, Parker KJ. Mouse liver dispersion for the diagnosis of early-stage Fatty liver disease: a 70-sample study. Ultrasound Med Biol 2014;40:704-13.
20. Sugimoto K, Moriyasu F, Oshiro H, Takeuchi H, Abe M, Yoshimasu Y, Kasai Y, Sakamaki K, Hara T, Itoi T. The Role of Multiparametric US of the Liver for the Evaluation of Nonalcoholic Steatohepatitis. Radiology 2020;296:532-40.
21. Sugimoto K, Lee DH, Lee JY, Yu SJ, Moriyasu F, Sakamaki K, Oshiro H, Takahashi H, Kakegawa T, Tomita Y, Abe M, Yoshimasu Y, Takeuchi H, Choi BI, Itoi T. Multiparametric US for Identifying Patients with High-Risk NASH: A Derivation and Validation Study. Radiology 2021;301:625-34.
22. Schulz M, Wilde AB, Demir M, Müller T, Tacke F, Wree A. Shear wave elastography and shear wave dispersion imaging in primary biliary cholangitis-a pilot study. Quant Imaging Med Surg 2022;12:1235-42.
23. Kambham N, Higgins JP, Sundram U, Troxell ML. Hematopoietic stem cell transplantation: graft versus host disease and pathology of gastrointestinal tract, liver, and lung. Adv Anat Pathol 2014;21:301-20.
24. Tian Y, Deng YB, Huang YJ, Wang Y. Bone marrow-derived mesenchymal stem cells decrease acute graft-versus-host disease after allogeneic hematopoietic stem cells transplantation. Immunol Invest 2008;37:29-42.
25. Tang Y, Kong W, Zhao J, Chen Y, Liu L, Zhang G. Can Viscoelasticity Measurements Obtained Through Shear-Wave US Elastography be used to Monitor Hepatic Ischemia-Reperfusion Injury and Treatment Response? An Animal Study. Ultrasound Med Biol 2020;46:2464-71.
26. Park SH, Lee SS, Sung JY, Na K, Kim HJ, Kim SY, Park BJ, Byun JH. Noninvasive assessment of hepatic sinusoidal obstructive syndrome using acoustic radiation force impulse elastography imaging: A proof-of-concept study in rat models. Eur Radiol 2018;28:2096-106.
27. Cooke KR, Kobzik L, Martin TR, Brewer J, Delmonte J Jr, Crawford JM, Ferrara JL. An experimental model of idiopathic pneumonia syndrome after bone marrow transplantation: I. The roles of minor H antigens and endotoxin. Blood 1996;88:3230-9.
28. Ferraioli G, Filice C, Castera L, Choi BI, Sporea I, Wilson SR, et al. WFUMB guidelines and recommendations for clinical use of ultrasound elastography: Part 3: liver. Ultrasound Med Biol 2015;41:1161-79.
29. Dietrich CF, Bamber J, Berzigotti A, Bota S, Cantisani V, Castera L, Cosgrove D, Ferraioli G, Friedrich-Rust M, Gilja OH, Goertz RS, Karlas T, de Knegt R, de Ledinghen V, Piscaglia F, Procopet B, Saftoiu A, Sidhu PS, Sporea I, Thiele M. EFSUMB Guidelines and Recommendations on the Clinical Use of Liver Ultrasound Elastography, Update 2017 (Long Version). Ultraschall Med 2017;38:e48.
30. Blatter DD, Crawford JM, Ferrara JL. Nuclear magnetic resonance of hepatic graft-versus-host disease in mice. Transplantation 1990;50:1011-8.
31. Ma SY, Au WY, Ng IO, Lie AK, Leung AY, Liang R, Lau GK, Kwong YL. Hepatitic graft-versus-host disease after hematopoietic stem cell transplantation: clinicopathologic features and prognostic implication. Transplantation 2004;77:1252-9.
32. Banff schema for grading liver allograft rejection: an international consensus document. Hepatology 1997;25:658-63.
33. Cleves MA. Comparative assessment of three common algorithms for estimating the variance of the area under the nonparametric receiver operating characteristic curve. The Stata Journal: Promoting communications on statistics and Stata 2002;2:280-9.
34. Lee DH, Lee JY, Bae JS, Yi NJ, Lee KW, Suh KS, Kim H,

Lee KB, Han JK. Shear-Wave Dispersion Slope from US Shear-Wave Elastography: Detection of Allograft Damage after Liver Transplantation. Radiology 2019;293:327-33.
35. Salomao M, Dorritie K, Mapara MY, Sepulveda A. Histopathology of Graft-vs-Host Disease of Gastrointestinal Tract and Liver: An Update. Am J Clin Pathol 2016;145:591-603.
36. Xin TY, Feng J, Chen SB, Chen X, Guo YY, Sun P, Chen YZ. Application of quantitative analysis of contrast-enhanced ultrasonography in the evaluation of acute radiation-induced liver damage. Exp Ther Med 2020;19:2957-62.

Cite this article as: Xiong Y, Xin Y, Liu F, Li W, Liu Y, Zhu J. Efficacy of shear wave dispersion imaging for viscoelastic assessment of the liver in acute graft-versus-host disease rats. Quant Imaging Med Surg 2022;12(11):5044-5055. doi:10.21037/qims-22-374